# In-Situ Navigation and Timing Services for a Human Mars Landing Site Part 2: System Design and Simulations[1]

Kar-Ming Cheung, Charles Lee
*Jet Propulsion Laboratory, California Institute of Technology, Pasadena, CA 91109, U.S.A.*

Glenn Lightsey, Ph.D.
*Georgia Institute of Technology, Atlanta, GA, 30332, U.S.A.*

**In a previous paper, we described the system concept of a proposed Mars Regional Navigation Satellite System (MRNSS) that is built upon a number of notional Mars orbiting and surface missions in the human exploration era of Mars. We assume two areostationary Mars relay orbiters that have continuous line-of-sight visibility with the Mars landing site, a Deep Space Habitat (DSH) in an inclined 48-hour circular orbit, and a surface communication lander that could serve as the reference point. These orbiting and surface infrastructure elements broadcast GPS-like ranging signals and other ephemeris information to the mission users. With one or more additional orbiters in areosynchronous orbits that trace around a figure-8 path, a regional navigation satellite system can be realized that provides in-situ course absolute localization and precision relative localization and timing services to the users in the vicinity of a Mars landing site.**

**We also introduced a new geometric trilateration method that simultaneously performs absolute positioning and relative positioning. The relative position is derived from a "differencing" function of two raw-range measurements between a known reference point and of the target from a navigation satellite, thereby eliminating most of the common errors like atmospheric delays, ephemeris errors, and instrument delays in real-time. In the Mars environment, this "error-cancellation" function greatly reduces the need to perform extensive orbit determination (OD) of the navigation satellites like the Earth's GPS, and only requires occasional tracks from the Earth's large-aperture deep space antennas to perform OD's.**

**In this paper, we provide detailed simulations on both the absolute positioning scheme and the relative positioning scheme, and show that the relative positioning scheme provides 200 – 400 times improvement in localization accuracy.**

**On the ground side, we discuss new approaches that simultaneously perform 2-way Doppler/ranging, and re-introduce the method of Same Beam Interferometry (SBI) for the Mars navigation orbiters. This helps to further reduce the tracking burden of the ground antennas required to support the OD of the Mars orbiters, making the concept of MRNSS more realizable.**

## I. Introduction

PLANNING for human Mars explorations requires substantial build-up of orbiting and surface infrastructures on Mars. In addition to communication coverage, location awareness would be essential to supporting various human and robotic activities on the Mars surface and on orbits. This includes localizing discoveries and returning to sites, construction and assembly of structures and habitats, entry/descent/landing, approach/rendezvous/docking, Mars ascent and orbit insertion, etc. It would therefore be desirable to establish a Mars Regional Navigation Satellite System (MRNSS) in the vicinity of the Mars landing site, similar to the Earth's Indian Regional Navigation Satellite System (IRNSS) [1]. The IRNSS consists of three navigation satellites in the Earth's geostationary orbits and four navigational satellites in geosynchronous orbits. The IRNSS provides continuous positioning and timing services to vehicles in the India and neighboring region with an absolute positioning accuracy of 10 meters. The IRNSS's ground segment

consists of four dedicated ground stations that perform 24/7 orbit determination (OD) measurements for the orbiting navigation satellites.

To provide accurate Mars surface positioning, the envisioned MRNSS requires precision OD of the orbiting Mars navigation nodes. The navigation nodes in MRNSS have to rely on the shared antennas of the Deep Space Network (DSN) and other space agencies. For a Mars orbiter, there are natural forces that tend to shift the spacecraft from its ideal trajectory predicted by the Kepler's Laws. The dominant factors are perturbations due to the non-spherical mass distribution of the Mars gravitational field, and the gravitational attraction of the Sun, Phobos, and Deimos moons. Solar radiation pressure also contributes to the disturbances. It is shown in [2] that long and continuous or near-continuous DSN tracking for 2 to 4 days is required to yield 10+ meters of OD errors for a Mars areostationary orbiter. This would translate into 10's or 100's of meters of localization error when the Earth-style GPS localization method is used. Apart from the impractical fact of tying up most of the DSN antenna resource to perform OD, this level of localization accuracy is insufficient for many activities for the orbiting and surface Mars assets.

In [3] and [4], we introduce a new geometric trilateration (GT) method that simultaneously performs absolute positioning and relative positioning. The relative position is derived from a "differencing" function of two raw-range measurements between a known reference point and of the target from a navigation satellite, thereby eliminating most of the common errors like atmospheric delays, ephemeris errors, and instrument delays in real-time. In the Mars environment, this "error-cancellation" function greatly reduces the need to perform extensive orbit determination (OD) of the navigation satellites like the Earth's GPS, and only requires occasional tracks from the Deep Space Network to perform OD's.

In [5], we described the system concept of the proposed MRNSS that is built upon a number of notional Mars orbiting and surface missions in the human exploration era of Mars. This constellation of Mars orbiters favors communication coverage, but offers poor geometry for navigation applications. In this paper, we provide simulations of the absolute and relative localization performance for a scenario of the human Mars landing site, and confirm the fact that relative positioning provides much better localization accuracy than absolute positioning in the presence of high OD errors of the Mars orbiters.

We also discuss new approach that simultaneously perform 2-way Doppler/ranging, and re-introduce Same Beam Interferometry (SBI) for the Mars navigation orbiters. This helps to further reduce the tracking burden of the ground antennas required to support the OD of the Mars orbiters, making the concept of MRNSS more realizable.

The rest of the paper is organized as follows: Section II describes the proposed MRNSS constellation that leverages on the two planned areostationary relay orbiters and the DSH in a circular 2-SOL inclined orbit, and augmented with a navigation satellite in a areosynchronous orbit that traces around a figure-8 path. Section III compares the accuracy performance of absolute positioning with relative positioning. Section IV introduces a new approach for a ground station that simultaneously perform 2-way Doppler/ranging with multiple spacecraft in the antenna beam. Section V describes how SBI can provide plane-of-sky measurements with multiple Mars orbiters that complement their Doppler measurements. Section VI provides concluding remarks and discusses future work.

## II. A Notional Mars Regional Navigation Satellite System (MRNSS)

We consider the scenario of a Human Mars landing site at Utopia Planitia on Mars, and propose a navigation satellite constellation that provides navigation and timing services in the surrounding region of the landing site. The navigation satellite constellation leverages on the two planned areostationary relay orbiters (Aero45 and Aero90) and the Deep Space Habitat (DSH) in a circular 48-hour inclined orbit (Mars48hr), and augmented it with a notional navigation satellite in a areosynchronous orbit that traces around a figure-8 path (Aero68). The notional Mars landing site location and orbiters' orbital parameters are given as follows:

| | |
|---|---|
| Utopia Planitia: | 182.5° due East, 46.7° due North |
| Aerostationary orbiter 1 (Areo45): | 162.5° due East |
| Aerostationary orbiter 2 (Areo90): | 207.5° due East |
| Aerosynchronous orbiter (Areo68): | 180° due East and 20° inclined |
| Deep Space Habitat (Mars48hr): | 180° due East, 149.5° inclined |

The orbits of the proposed Mars navigation nodes are shown in Figure 1 (3-D view), and the projections of these orbits onto the Mars surface are shown in Figure 2 (2-D view). Note that in Figure 2 the Mars navigation nodes cluster together, and Utopia Planitia is north of the cluster. The satellite-receiver geometry appears to be weak and the Position Dilution of Precision (PDOP) is high. In other words, the localization solution can be very sensitive to the errors in the raw-range measurements. The detailed system concept is described in [5].

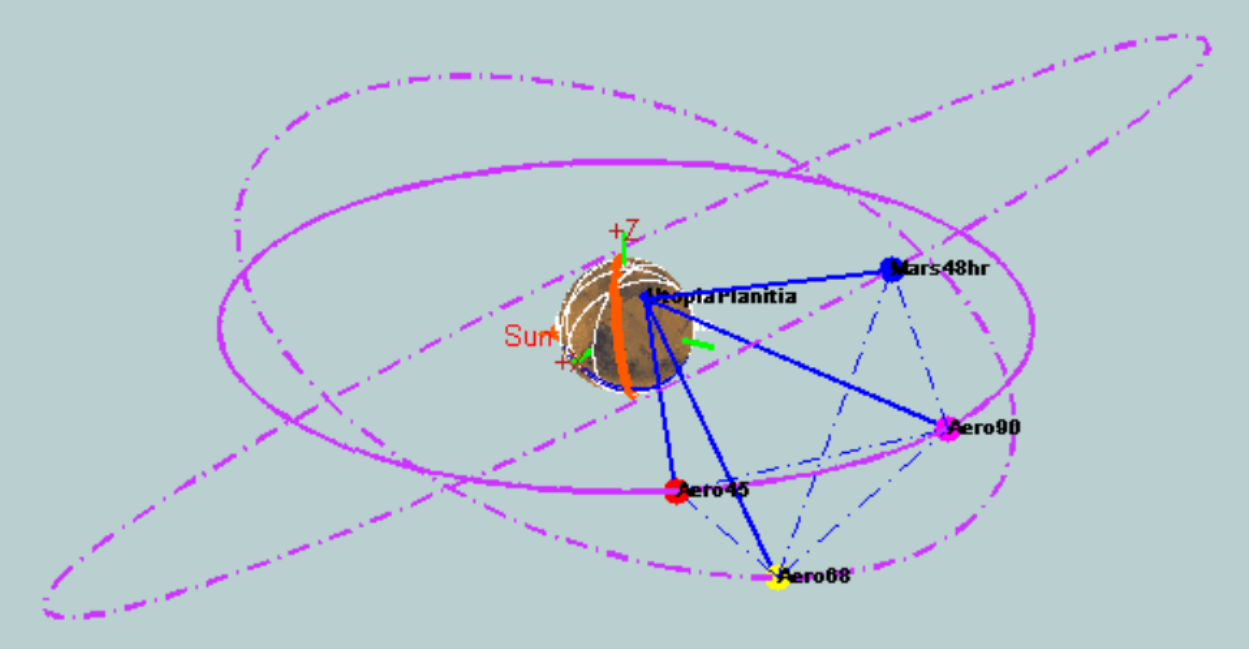


**Fig. 1 Orbits of the Notional Mars Navigation Nodes (3-D View).**

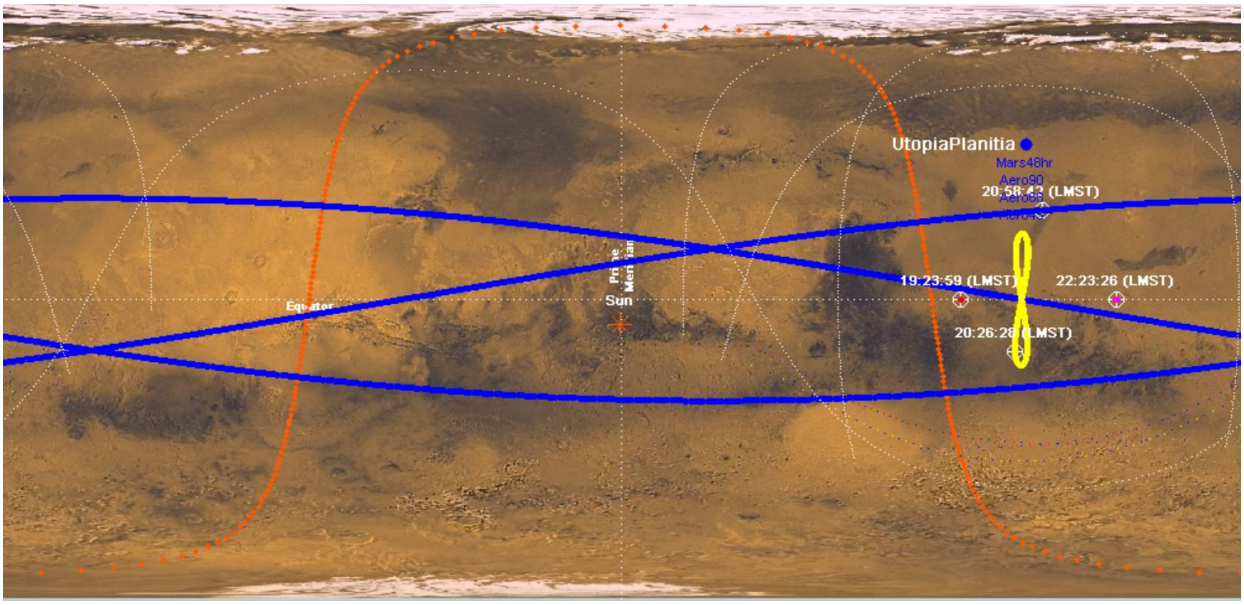


**Fig. 2 Orbits of the Notional Mars Navigation Nodes (2-D View).**

## III. Comparison of Localization Accuracy between Absolute and Relative Positioning

Note that Utopia Planitia and the two areostationary orbiters are fixed in the Mars Center Mars Fixed (MCMF) Cartesian coordinate. Using the above Mars landing site location and orbiters' orbital parameters, we consider a time instance when the areosynchrous orbiter and the DSH are at locations (-19191.34, 0.00, 6985.08) and (-27460.98, 0.00, 6985.08) respectively (units are in kilometers). This satellite geometry as viewed by Utopia Planitia, has a high PDOP of 113.17.

A position solution was obtained using both algorithms for 10,000 simulations of the Martian position described in the previous section with the statistical receiver noise errors for pseudo-range and each navigation node location. A range of different error conditions is shown for pseudo-range measurement error $\sigma_r$ from 0 to 5.0 cm and navigation node position error $\sigma_v$ from 0 m to 35 m. A receiver clock offset of $\Delta t$ = 10 microseconds was included in every

simulation. The absolute localization accuracy performance is given in Table 1, and the relative localization accuracy performances for the cases when the vehicle is 100 km and 10 km away from the reference site are given in Tables 2 and 3 respectively.

| Our Proposed Scheme | | GPS Satellite Position Error | | | | | | | |
|---|---|---|---|---|---|---|---|---|---|
| | | 0m | 0.5m | 1m | 2m | 5m | 10m | 30m | 35m |
| Pseudo-range error | 0 cm | 0.00 | 3273.85 | 6547.69 | 13095.39 | 32738.48 | 65476.99 | 196431.3 | 229169.9 |
| | 0.10 cm | 11.27 | 3273.70 | 6547.54 | 13095.23 | 32738.32 | 65476.82 | 196431.1 | 229169.7 |
| | 0.25 cm | 28.19 | 3273.56 | 6547.35 | 13095.01 | 32738.08 | 65476.58 | 196430.9 | 229169.5 |
| | 0.50 cm | 56.37 | 3273.51 | 6547.12 | 13094.69 | 32737.71 | 65476.19 | 196430.5 | 229169.1 |
| | 1.00 cm | 112.74 | 3274.15 | 6547.03 | 13094.24 | 32737.04 | 65475.45 | 196429.7 | 229168.3 |
| | 2.00 cm | 225.48 | 3278.35 | 6548.30 | 13094.06 | 32735.98 | 65474.10 | 196428.1 | 229166.7 |
| | 5.00 cm | 563.71 | 3313.95 | 6563.76 | 13099.34 | 32735.15 | 65471.23 | 196423.9 | 229162.4 |

Table 1. $\sigma_{3D}$ Absolute Localization Error standard deviation (cm) of the New Scheme. PDOP=113.17.

| Our Proposed Scheme | | GPS Satellite Position Error | | | | | | | |
|---|---|---|---|---|---|---|---|---|---|
| | | 0m | 0.5m | 1m | 2m | 5m | 10m | 30m | 35m |
| Pseudo-range error | 0 cm | 14.43 | 21.57 | 35.07 | 65.44 | 160.06 | 319.04 | 956.04 | 1115.33 |
| | 0.10 cm | 21.59 | 26.82 | 38.47 | 67.27 | 160.75 | 319.32 | 956.05 | 1115.32 |
| | 0.25 cm | 42.77 | 45.58 | 53.22 | 76.58 | 164.76 | 321.27 | 956.58 | 1115.75 |
| | 0.50 cm | 81.89 | 83.33 | 87.69 | 103.45 | 178.67 | 328.48 | 958.82 | 1117.63 |
| | 1.00 cm | 161.95 | 162.62 | 164.84 | 173.62 | 226.38 | 356.41 | 968.34 | 1125.72 |
| | 2.00 cm | 323.00 | 323.28 | 324.34 | 328.78 | 359.12 | 452.05 | 1006.71 | 1158.71 |
| | 5.00 cm | 806.95 | 806.99 | 807.34 | 808.99 | 821.36 | 865.36 | 1246.30 | 1371.59 |

Table 2. $\sigma_{3D}$ Relative localization Error standard deviation (cm) of the New Scheme. Distance between reference and target = 100 km. Sigma = 100 m. Delta = 100 m.

| Our Proposed Scheme | | GPS Satellite Position Error | | | | | | | |
|---|---|---|---|---|---|---|---|---|---|
| | | 0m | 0.5m | 1m | 2m | 5m | 10m | 30m | 35m |
| Pseudo-range error | 0 cm | 0.14 | 1.59 | 3.18 | 6.35 | 15.87 | 31.73 | 95.20 | 111.07 |
| | 0.10 cm | 16.03 | 16.10 | 16.32 | 17.20 | 22.47 | 35.45 | 96.42 | 112.10 |
| | 0.25 cm | 40.08 | 40.10 | 40.18 | 40.53 | 42.99 | 50.93 | 103.02 | 117.79 |
| | 0.50 cm | 80.15 | 80.16 | 80.19 | 80.36 | 81.59 | 85.99 | 123.99 | 136.48 |
| | 1.00 cm | 160.31 | 160.30 | 160.32 | 160.39 | 160.97 | 163.19 | 185.83 | 194.34 |
| | 2.00 cm | 320.62 | 320.61 | 320.61 | 320.63 | 320.89 | 321.95 | 333.77 | 338.52 |
| | 5.00 cm | 801.54 | 801.53 | 801.52 | 801.52 | 801.58 | 801.93 | 806.47 | 808.38 |

Table 3. $\sigma_{3D}$ Relative localization Error standard deviation (cm) of the New Scheme. Distance between reference and target = 10 km. Sigma = 100 m. Delta = 100 m.

It is instructive to consider the absolute localization error performance for several of the cases that are listed in Table 1. In the upper left corner, it is seen that when both the navigation node error and the pseudo-range error are zero, the algorithm determines the correct position as expected. In the leftmost column of the Table 1, when the pseudo-range position error is given by $\sigma_r = 1.0$ cm, the standard deviation of the 3D localization error is $\sigma_{3D}$=112.74 cm. This value is very close to the theoretically predicted localization accuracy by the position dilution of precision (PDOP). Also, it is noted that for navigation node position errors as small as $\sigma_v = 0.5$ m, the 3D localization errors $\sigma_{3D}$ expand to 30+ meters irrespective of the pseudo-range measurement errors, and $\sigma_{3D}$ scales approximately linearly with the navigation node standard deviation $\sigma_v$.

On the other hand, in Tables 2 and 3, the 3D localization errors are a lot more immune to the navigation node position errors. For $\sigma_v$ as high as 5m, which is the typical OD accuracy of DSN, $\sigma_{3D}$ is 1 – 2m for relative positioning when the vehicle is 100 km from the reference, and is less than a meter when the vehicle is 10 km from the reference.

This confirms the intuition that relative positioning helps to eliminate much of the common errors that include the navigation node position errors, thus greatly reduce the need to perform extensive orbit determination (OD) of the navigation satellites.

## IV. Simultaneous 2-Way Doppler/Ranging for Multiple Spacecraft

In this paper, we leverage on prior work [6] that focuses on simultaneous command and telemetry links, and introduces a new flight-ground collaborative architecture that provides simultaneous Doppler and ranging for multiple spacecraft in the Mars vicinity. We assume that 2-way ranging is done in X-band, which also supports low-rate command and telemetry. The operational Deep Space Network (DSN)'s Multiple-Spacecraft-Per-Antenna (MSPA) method is basically static Frequency Division Multiple Access (FDMA) scheme. For *N* Mars orbiters, the downlinks operate in *N* allocated frequency bands separated by *N-1* guard bands to prevent interferences. On the other hand, the uplinks received by the N orbiters exhibit different Doppler and Doppler rate effects due to their different dynamics with respect to Earth.

To enable simultaneous Doppler and ranging measurements, we propose the following updates to the existing flight and ground systems and the frequency allocation process:

1. The *N* spacecraft time share a single uplink frequency – we assume that each spacecraft is capable of acquiring and tracking the same Doppler-compensated uplink (to be discussed later), which is shared among all spacecraft. This approach on uplink was also recommended for the Multiple-Uplink-Per-Antenna (MUPA) concept [7].
2. The ground "Doppler-compensates" the uplink signal in some "average" way with respect to the N orbiters such that each orbiter would not experience excessive high Doppler and Doppler rate residuals.
3. On the spacecraft side, the Command and Data Handling (C&DH) subsystem of each spacecraft has to be able to identify its own uplink commands and data loads on the uplink data stream using its unique spacecraft Identifier (SCID). The onboard radio would require the following upgrades:
    a. A different turn-around-ratio for each spacecraft so that the same Doppler-compensated uplink signal received by each spacecraft would be coherently "turned-around" to modulate the telemetry and ranging signals on a different downlink frequency.
    b. A well-designed tracking loop that can sweep, acquire, and track the unknown uplink carrier phase and residual Doppler frequency. A preliminary design of this type of tracking loop was introduced in [8] for use by a constellation of 20 spacecraft in a halo orbit around the Earth-Moon Lagrange Point L1.
4. On the frequency allocation side, the guard bands have to be wide enough to ensure that adjacent ranging signals do not interfere with one another.
5. On the ground side, no ground processing equipment needs modification, but *N* Receiver Ranging Processors (RRP's) are needed to acquire and to track the *N* streams of Doppler frequencies and ranging signals. The range measurement technique for deep space spacecraft is described in details in [9].

### A. Doppler and Doppler Rate Simulation for the Proposed MRNSS Constellation

We assume 2-way Doppler and ranging are done in X-band. For the proposed scheme of transmitting one uplink signal to multiple spacecraft, each spacecraft experiences different Doppler and Doppler rate effects due to their different dynamics relative to the Earth's ground station. We propose the following collaborative flight-ground architecture for simultaneous 2-way Doppler and ranging: the ground antenna "Doppler compensates" the uplink carrier signal with either one of the following ways: i) with respect to the Mars center, or ii) with respect to the average of Doppler profiles of all the spacecraft. This ensures that the residual Doppler frequencies and Doppler rates as experienced by all the spacecraft are comparable. On the flight side, the radio on each spacecraft sweeps, acquires, and tracks the unknown uplink carrier phase and residual Doppler frequency. Using the above proposed MRNSS scenario, we simulate the Doppler's and Doppler rates of the four orbiters and the landing site Utopia Planitia for 8 days, and compare with the Doppler frequencies and Doppler rates of the Mars center and the Doppler centroid. A 30-hour time profile of the simulations is shown in Figure 3. The maximum residual Doppler and Doppler rate as experienced by each spacecraft using the Doppler compensation strategies of i) Mars center and ii) Doppler centroid are shown in Figures 4 and 5 respectively.

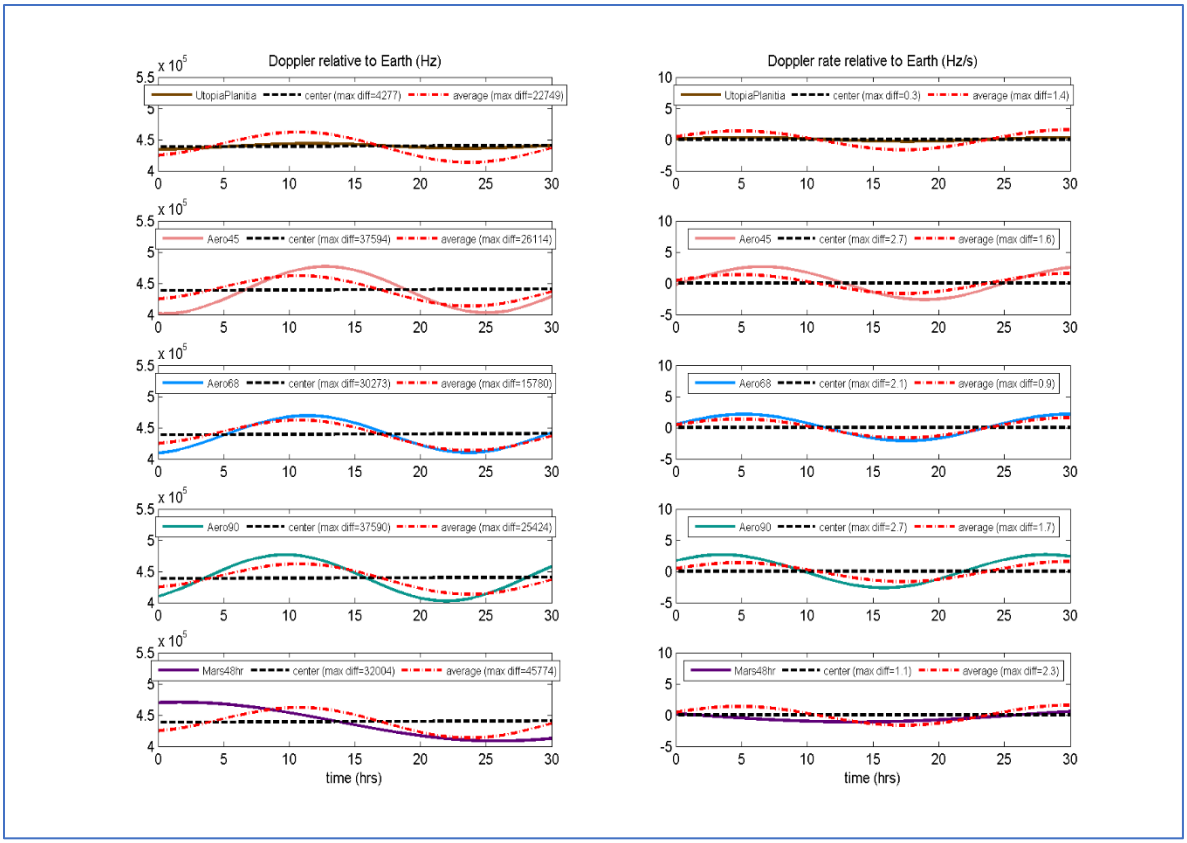


**Fig. 3 30-Hour Time Profiles of Doppler and Doppler Rate.**

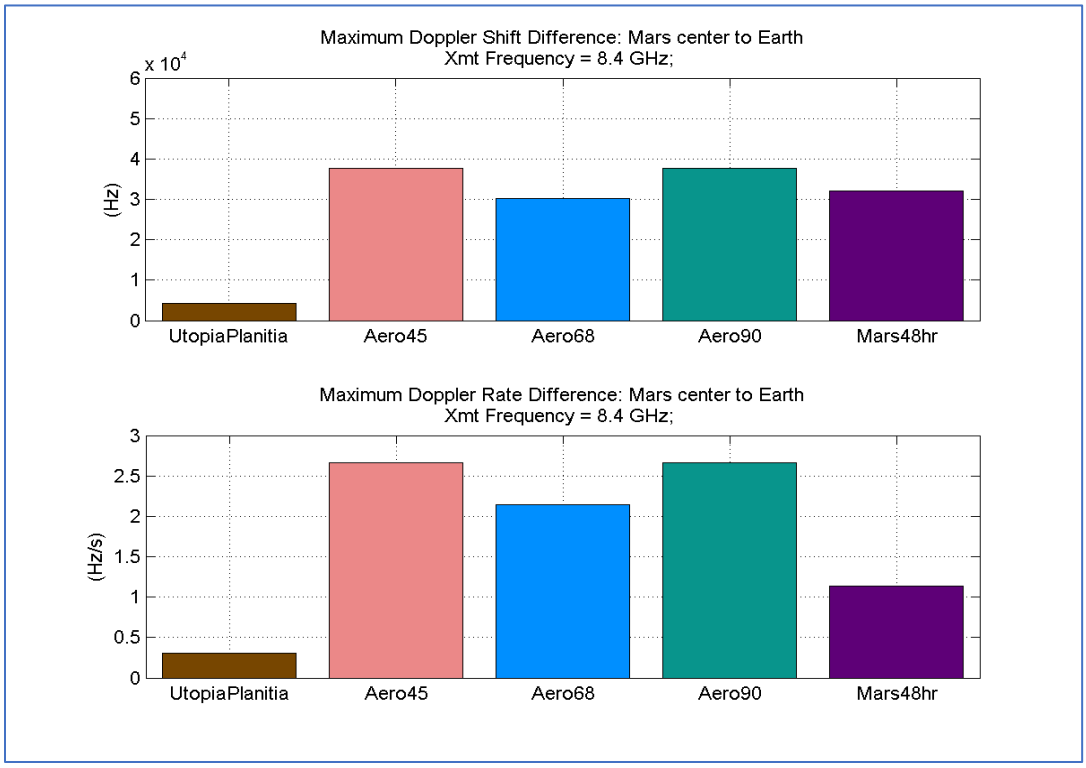


**Fig. 4 Maximum Residual Doppler/Doppler Rate with Mars Center Compensation Strategy.**

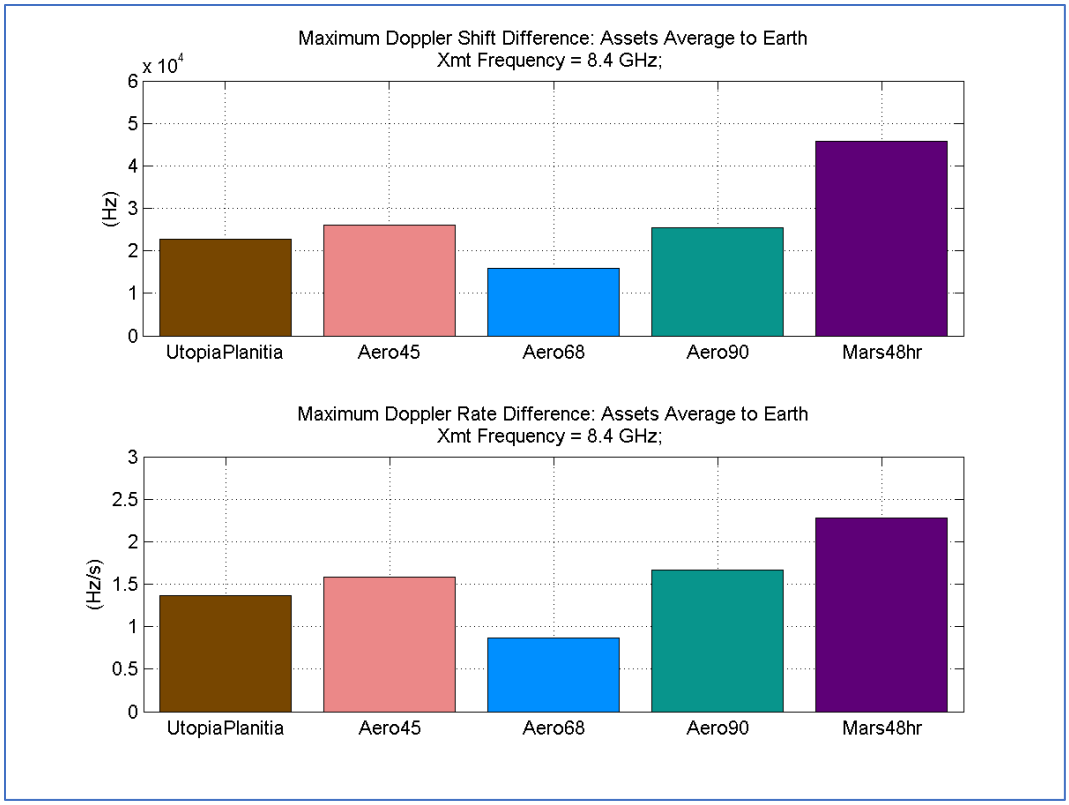


**Fig. 5 Maximum Residual Doppler/Doppler Rate Using Doppler Centroid Compensation Strategy.**

### B. Proposed Flight Tracking System

To acquire and to tracking an uplink carrier with high unknown residual Doppler and Doppler rates, we propose to use a Phase Lock Loop (PLL) with smart sweeping algorithm. The schematic of a spacecraft receiver that includes a PLL with controlled sweeping frequency is shown in Figure 6. The frequency acquisition algorithm that controls the frequency sweep requires the range of frequency sweep to be defined through a start frequency $f_1$, a final frequency $f_2$, and a frequency step size $f_{step}$ to increment the frequency. The frequency step size is usually between ¼ and ½ of the tracking loop bandwidth. Additionally, a threshold "Th" for lock detection should be defined. The parameter *P* as shown in Figure 6 is obtained by integrating *N* magnitude of samples after mixer during each frequency interval. The parameter *N* should be chosen to maintain the lock stability.

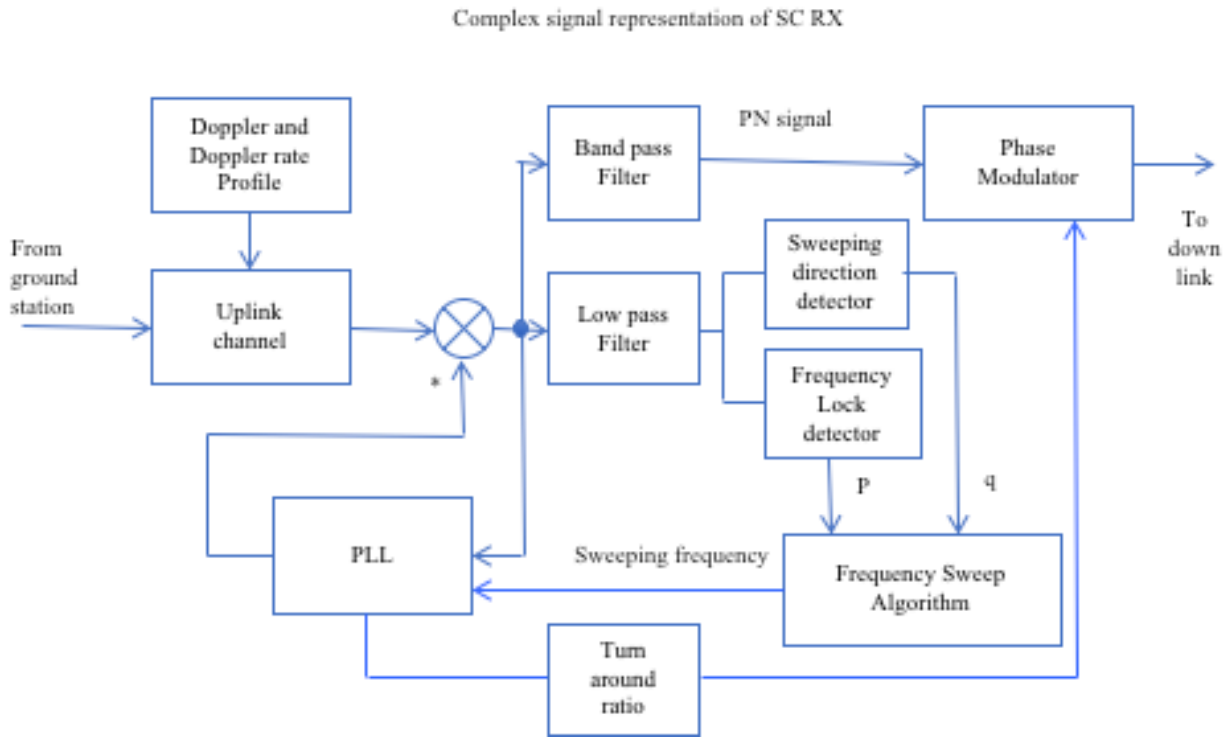


**Fig. 6 Spacecraft Receiver that Includes PLL with Frequency Sweep**

Many existing flight radios use simple sweeping algorithms with a single threshold "Th", a single step size $f_{step}$, and one sweeping direction (low-to-high), e.g. Electra radio [10][11]. We propose a smart sweeping algorithm with the following enhancements:

1. Use multiple thresholds, and change $f_{step}$ when P exceeds a certain threshold.
2. Compare the received frequency $f_{RX}$ and the PLL frequency $f_{PLL}$ to determine the frequency sweep direction.

The smart sweeping algorithm is shown in Fig. 7, and preliminary simulation results as shown in Figure 8 indicate that this approach achieve fast acquisition of carrier frequency with high unknown residual Doppler and Doppler rate. A more comprehensive treatment of the above simultaneous 2-way Doppler/ranging tracking methods is given in another paper in this conference [20]. Optimal tuning of thresholds and step sizes under different operation environment is underway.

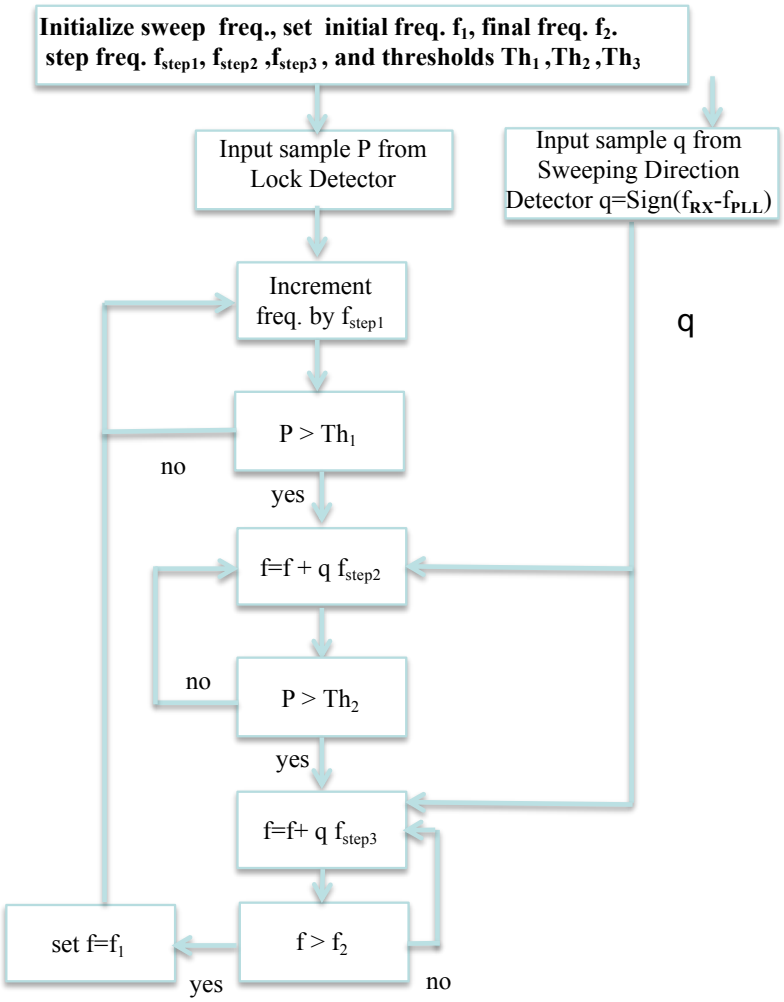


**Fig. 7 Smart Sweeping Algorithm.**

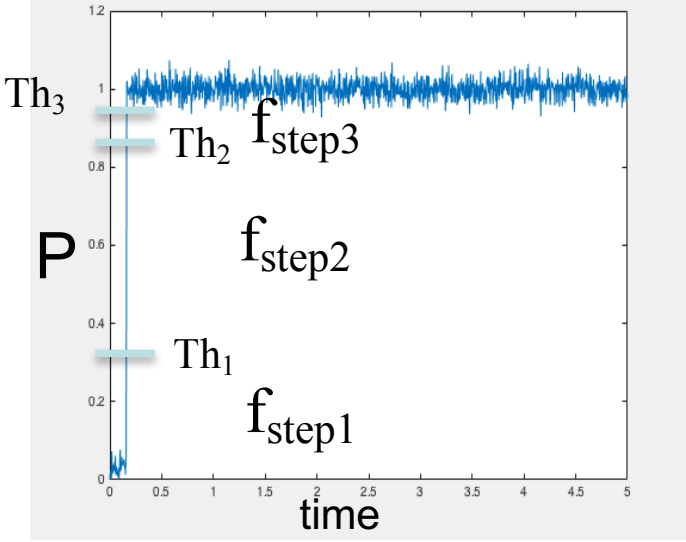


**Fig. 8 Frequency Acquisition Thresholds, Step Sizes, and Performance.**

## V. Same Beam Interferometry

The 2-way Doppler and ranging techniques discuss in the last Section infer orbit parameters from signature in line-of-sight data. Very Long Baseline Interferometry (VLBI) techniques estimate angle of arrival by measuring the difference in the signal time of arrival at two ground stations that are far-apart (thus very long baseline). This measurement provides plane-of-sky measurements that complement Doppler [12]. The raw delay measurements include errors like station clock offsets, instrument delays, media effects, and poorly modelled baseline vectors.

Delta VLBI reduces the above errors by introducing a second measurement, that of an angularly nearby quasar whose position is known to a high degree of accuracy. By taking the differences between the two delay measurements, much of the common errors would be eliminated depending on how angularly close between the spacecraft and the quasar. During delta VLBI operation when a spacecraft is tracked by two 34-m Beam Waveguide (BWG) antennas, the antennas have to point back and forth between the spacecraft and the quasar for a brief period of time which can be operationally tedious.

For two orbiters around Mars, they are so close angularly that they are in the same beams of the two Earth-based 34-m BWG antennas. Differential interferometric observables may be generated using simultaneous observations of the two spacecraft from two 34-m BWG antennas. This technique is known as Same Beam Interferometry (SBI), and has the following advantages:

1. SBI simplifies operation as this technique does not require constantly toggling between a quasar and a spacecraft, thus increases the effective observation time in a pass.
2. As the angular distance between two Mars orbiters is much smaller than the angular distance between a quasar and a spacecraft, SBI provides much more accurate relative angular measurements in the plane-of-the-sky.

Improved OD using SBI was demonstrated with the Pioneer Venus and Magellan orbiters at Venus [13][14]. SBI was also used or proposed for use in various deep space missions including lunar missions [15 – 18]. For multiple orbiters at Mars, SBI could be used to improve OD while requiring fewer Earth-based tracking resources. All spacecraft within Mars areostationary orbit would be visible within the 1-mrad beamwidth of a 34-m BWG antenna at X-band. All signals would be acquired simultaneously.

We performed covariance analysis of the orbiter nodes in the aforementioned MRNSS constellation and showed that SBI and 2-way Doppler improves OD accuracy (in RMSE sense) by a factor of 2 – 10 [19].

## VI. Concluding Remarks and Future Work

In this paper, we report on the progress of our investigation on a proposed low-cost, low-maintenance regional navigation satellite system architecture that would provide in-situ navigation and timing services for the robotics and human missions in the vicinity of the Mars landing site. We provide simulations of the absolute and relative localization performance for a scenario of the human Mars landing site, and confirm the fact that relative positioning provides much better localization accuracy than absolute positioning in the presence of high OD errors of the Mars orbiters.

We also introduce new approaches that simultaneously perform 2-way Doppler/ranging and Same Beam Interferometry (SBI) for the Mars navigation orbiters. This helps to further reduce the tracking burden of the ground antennas required to support the OD of the Mars orbiters, making the concept of MRNSS more realizable.

In the near-future, we plan to investigate the signal design and carrier-phase ranging system of the navigation satellites. One challenge of the MRNSS scenario is the poor geometry and the lack of orbital dynamics with respect to the Mars surface assets. A lot of work has been done in Earth's global navigation satellite system (GNSS) area. We plan to leverage on the Earth's established navigation techniques, but tailored them to perform real-time high-accuracy localization in the human Mars landing site environment. Examples are: dual and triple frequency receivers to improve navigation performance, fast integer ambiguity resolution techniques for carrier-phase tracking, etc.

On the ground side, we will continue to refine the simultaneous 2-way Doppler/ranging techniques by introducing smart but implementable frequency sweeping logics on the flight radio. This includes optimal tuning of thresholds and step sizes under different operation environment, and the heuristics as on when to change direction of frequency search. For SBI, we will investigate the feasibility of making SBI a routine ground network operational technique. We also started to consider extension of SBI from one baseline to multiple baselines. Preliminary results show that when the geometry is right, by using two simultaneous baselines SBI enables highly accurate angular distance estimation between two spacecraft based on double-differencing of signal arrival times. This enable new mission concepts in distributed spacecraft localization and radar applications. The new results will be reported in some future papers.

## Acknowledgement

This research was carried out at the Jet Propulsion laboratory, California Institute of Technology, under a contract with the National Aeronautics and Space Administration.

## References

[1] R. Shriwas, R. Bele, R. Kalaskar, and P. Jaiwsal, "Indian Regional Navigation Satellite System," International Journal of Research In Science & Engineering, Special Issue: Techno-Xtreme 16, April 2016.

[2] P. Romero et. al., "Analysis of orbit determination from Earth-based tracking for relay satellites in a perturbed areostationary orbit, Acta Astronautica, 136 (2017) 434-442.

[3] K. Cheung, C. Lee, "A Trilateration Scheme for Relative Positioning," IEEE Aerospace Conference 2017, Big Sky, Montana, March 2017.

[4] K. Cheung, C. Lee," A Trilateration Scheme for GPS-Style Localization," Interplanetary Network Progress Report, 42-209, May 2017.

[5] K. Cheung, C. Lee, "In-Situ Navigation and Timing Services for a Human Mars Landing Site Part 1: System Concept," September 2017, 68th International Astronautical Congress, Adelaide, Australia.

[6] D. Abraham et. al., "Enabling Affordable Communications for the Burgeoning Deep Space CubeSat Fleet," SpaceOps 2016, Daejeon, S. Korea, May 2016.

[7] D. Abraham et. al., "Deep Space Capacity Study – Pass 2," JPL internal report.

[8] D. Divsalar, K. Cheung, et. al., "CDMA Communication System Performance for a Constellation of CubeSats around the Moon," IEEE Aerospace Conference 2016, Big Sky, March 2016.

[9] J. Berner, S. Bryant, and P. Kinman, "Range Measurement as Practiced in the Deep Space Network," Proceedings of the IEEE, Vol. 95, No. 11, November 2007.

[10] C. D. Edwards, T. C. Jedrey, E. Schwartzbaum, A. S. Devereaux, R. De-Paula, M. Dapore, and T. W. Fischer, "The Electra proximity link payload for Mars relay telecommunications and navigation, IAC-03-Q.3.A06," in International Astronautical Congress 2003 , Sep.-Oct. 2003.

[11] "Autonomous Software-Defined Radio Receivers for Deep Space Applications," Jon Hamkins (Editor), Marvin K. Simon (Editor), Joseph H. Yuen (Series Editor),ISBN: 978-0-470-08212-6, Oct 2006, John Wiley & Sons.

[12] C. Thornton, J. Border, "Radiometric Tracking Techniques for Deep-Space Navigation," Monograph 1, Jet Propulsion Laboratory, California Institute of Technology, Pasadena, CA. http://descanso.jpl.nasa.gov/Monograph/series1/Descanso1_all.pdf.

[13] J. Border, W. Folkner, et. al. "Precise Tracking of the Magellan and Pioneer Venus Orbiters by Same-Beam Interferometry, Part I: Data Accuracy Analysis," TDA Progress Report, 42-110, vol. April – June 1992.

[14] W. Folkner, J. Border, et. al. "Precise Tracking of the Magellan and Pioneer Venus Orbiters by Same-Beam Interferometry, Part II: Orbit Determination Analysis," TDFA Progress Report, 42-113, vol. January – March 1993.

[15] Q. Liu, F. Kikuchi, K. Matsumoto, et. al., "Error Analysis of Same-Beam Differential VLBI Technique using two SELENE satellites," Advances in Space Research 40 (2007).

[16] M. Chen, Q. Liu, "Study on Differential Phase Delay Closure of Same-Beam VLBI," 2nd International Conference on Computer Engineering and Technology, April 2010, Chengdu, China.

[17] S. Chen, Q. Liu, "A Study on Accurate Same Beam Interferometry Differential Phase Delay Closure," 12th International Conference on Computer and Information Technology, October 2012, Chengdu, China.

[18] T. Martin-Mur, D. Highsmith, "Mars Approach Navigation Using the VLBA," Proceedings of the 21st International Symposium on Space Flight Dynamics, Toulouse, France, September 28 – October 2, 2009.

[19] T. Martin-Mur, J. Border, K. Cheung, "Mars Orbiter Same Beam Interferometry Covariance Analysis," to be published.

[20] K. Cheung, D. Divsalar, "Simultaneous Two-Way Doppler and Ranging for Multiple Spacecraft at Mars: Flight Radio Tracking System Design and Performance Simulations," to be presented in SpaceOps 2018, Marseille, France, May 28 – June 1, 2018.